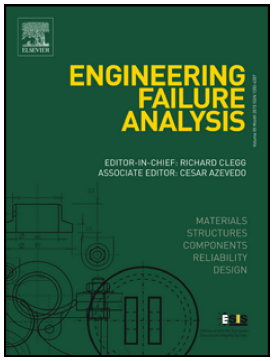

Failure analysis of a special vehicle engine connecting rod

Slavko Rakić, Ugljesa Bugaric, Igor Radisavljevic, Zeljko Bulatovic

PII: S1350-6307(16)30719-1
DOI: doi: 10.1016/j.engfailanal.2017.04.014
Reference: EFA 3094

To appear in: *Engineering Failure Analysis*

Received date: 24 August 2016
Revised date: 11 February 2017
Accepted date: 19 April 2017

Please cite this article as: Slavko Rakić, Ugljesa Bugaric, Igor Radisavljevic, Zeljko Bulatovic , Failure analysis of a special vehicle engine connecting rod. The address for the corresponding author was captured as affiliation for all authors. Please check if appropriate. Efa(2017), doi: 10.1016/j.engfailanal.2017.04.014

Failure analysis of a special vehicle engine connecting rod

Corresponding author:
MSc Slavko Rakić, technical service officer
Sector for Material Resources
Ministry of Defence of Republic of Serbia,
Nemanjina 15, 11000 Belgrade, Serbia.
phone: +381 11 2059 227
fax: +381 11 3006 221
e-mail: slavko.rakic@mod.gov.rs

Other authors:
Dr Ugljesa Bugaric, professor,
Department of Industrial Engineering,
Faculty of Mechanical Enginering Belgrade,
University of Belgrade
Kraljice Marije 16, 11000 Belgrade, Serbia
e-mail: ubugaric@mas.bg.ac.rs
phone: +381 11 3302347
fax: +381 11 3370364

Dr Igor Radisavljevic, researcher,
Military Technical Institute
Division for materials and protection
Ministry of Defence of Republic of Serbia
Ratka Resanovica 1, 11000 Belgrade, Serbia
e-mail: igor.radisavljevic@vti.vs.rs
phone:; +381 11 2051278
fax: +381 11 2508474

Dr Zeljko Bulatovic, researcher,
Military Technical Institute
Division for engines and vehicle
Ministry of Defence of Republic of Serbia
Ratka Resanovica 1, 11000 Belgrade, Serbia
e-mail: zetonbulat@gmail.com
phone: +381 62 8122876

Abstract

This paper presents failure analysis of the connecting rod used in a 12-cylinder diesel engine set on a special vehicle. The fracture of the connecting rod occurred during the engine test in laboratory conditions. Chemical and metallographic analysis as well as mechanical testing have confirmed that the material properties of the connecting rod met the requirements of standard specification and technical documentation. Linear finite element (FE) analysis was performed to evaluate stress state of the connecting rod under maximum load. The results of FE analysis showed that the position of the fracture is consistent with the zone of highest stress. Fractographic analysis has not been able to reveal the main cause of mechanism of fracture due to substantially damaged fracture surface.

Inadequate machining, absence of polishing and highest stress in the region of fracture were identified as the main causes of failure. Finally, the engine had been working at maximum load for a longer period of time that also led to the breakage of the connecting rod.

1. Introduction

The connecting rod is an element of the internal combustion engine that transmits motion and forces amongst the piston and crankshaft. Due to the cyclical nature of internal combustion (IC) engine work process, all moving elements are subjected to variable loads and change in the direction of motion.

The body of the connecting rod is dominantly loaded against the pressure of the gas force and the tensile force due to inertial forces. Both the maximum gas force and maximum value of the inertial force occur in the expansion stroke. These forces generate the minimum and maximum normal stress within the cross-section of the body of the connecting rod.

Connecting rods as well as other mechanical parts, which are exposed to variable load, are dimensioned to meet the durable dynamic strength. The dynamic strength is subject to the influence of several parameters. In this case, the condition of the connecting rod surface and material properties are crucial. A fracture of the connecting rod in the running engine leads to a complete stop of the engine. The same occurrence can lead to catastrophic consequences in other engine designs.

In the previous research, the study of the connecting rod failure was carried out in many ways.

Rabb [1] analyzed fatigue failure of a connecting rod in a medium-speed diesel engine. The difficulties in making a sufficient FE model with exact geometric details and important nonlinearities are explained. Fatigue tests of the connecting rod material were also carried out. The FE analysis and fatigue data resulted in an overall design improvement of the connecting rod.

Bai-yan He et al. [2] described the failure of a connecting rod used in a diesel generator that was set on an offshore platform. The cracks occurred on the toothed mating surface of the connecting rod after approximately 6,000-10,000 hours in service. Based on such results, a conclusion was drawn that the main cause of failure in the connecting rod was due to a lower yield of material's strength and high level of stress concentration.

Khare et al. [3] investigated the reason for the occurrence of damage on a spalling form connecting rod. The users of the vehicle reported a high noise and vibration in the engine at an early stage of the service lifetime. The results show high interfacial pressure and stresses near the junction of the web and the flange of the connecting rod. The modified design of the connecting rod shows a significant reduction in the extreme pressure in FE model, resulting in a significant enhancement of durability in laboratory test. A discussion about the spalling problem has been provided, leading to the connection of the pick pressure and the spalling phenomena.

Griza et al. [4] performed the fracture analysis consists of microstructure analysis and numerical simulation of the fracture mechanics on connecting rod bolts.

Son et al. [5] used the flexible multi-body dynamic analysis in combination with the elasto-hydrodynamic model to calculate the actual force acting on the mating surface of the connecting rod and predicted the possibility of fretting damage.

The investigated connecting rod is made of high-quality alloy steel 18H2N4MA. This steel has excellent mechanical properties at elevated temperatures, but is sensitive to stress concentration [6]. Therefore, the technical documentation specifies that the complete surface of the connecting rod should be in a polished condition. The treatment of the connecting rod surface by polishing is also applied in order to increase the dynamic strength without dimensional adjustments.

1.1. Problem situation

During the laboratory tests conducted on the 12-cylinder diesel engine, there was an engine breakdown due to the fracture of the connecting rod of the first left cylinder of the engine, Fig. 1. The projected life span of the subject-matter engine is 500 hours of operation, whereas the engine had 130 hours of operation until the breakdown and 5 hours of operation on the engine test bench in the testing laboratory. The last regular periodic check of the engine was carried out 10 hours before the breakdown and a conclusion was drawn that all the parts of the engine and its systems were functioning properly.

The engine specifications are presented in Table 1.

All the control parameters of the engine: the temperatures of the oil, the coolant and the exhaust gas, as well as the pressures of the air, the oil and the gases in the crankcase were within the acceptable limits

during the engine test. These parameters were read and recorded in the test protocol every 15 minutes during the running of the engine.

The last record of the measured values was made at the beginning of the fourth hour of the engine running at maximum load and the number of the revolutions n = 1800 rpm, just before the tests were stopped because of the engine breakdown. All the control values were within the given limits.

In a short period after the connecting rod had been fractured, the uncontrolled movement of its part, which remained contact with the crankpin journal of the engine crankshaft, caused the greatest damage to the engine. Firstly, this part of the connecting rod penetrated through the lower part of the crankcase engine and dislocated the oil pump from its position in the oil pan. Secondly, it broke the upper part of the crankcase of the engine in the area of the front left support of the engine. Then, it smashed the free end of the cylinder liner and, finally, plunged into the ridge of cylinder block. This ridge was found deformed with a visible crack.

The additional damage was caused by the uncontrolled movement of the auxiliary connecting rod and the piston of the first cylinder on the right. The surface of the fracture on the part of the connecting rod which is connected to the piston with the small end - Fig. 2- is significantly deformed due to the multiple collisions with the other part of the connecting rod, until the time when the engine was stopped.

2. Failure analysis procedure

Failure analysis was used to determine the root causes of the engine breakdown, with a special emphasis on the determination of the causes that led to the failure of the connecting rod.

After removing the engine from the test bench, a visual overview of the broken connecting rod, the engine parts and the assemblies, as well as the correctness of the fuel injectors was elaborated. The fractured connecting rod was subjected to the external visual inspection by the unaided human eye in the received condition.

The next step was a detailed fractographic analysis of the fracture surfaces. The macrofractographic examination was carried out in order to detect the crack origin location on the broken connecting rod, providing information about the failure mechanism and the most interesting areas for a further analysis. The macroscopic analysis of the fracture surface was carried out on the Leica M205A stereomicroscope, equipped with a computer system and software for image acquisition and data processing. The fracture surfaces were previously ultrasonically cleaned. After that, the fracture surface was analyzed using the high performance scanning electron microscope (SEM) JEOL JSM-6610LV.

In order to determine the extent of machining, surface roughness was investigated. Testing was done on the Taylor-Hobson Surtronic 3 device for roughness measurement.

In order to check the quality of the material of the connecting rod, an analysis of the chemical composition, as well as the structural and mechanical testing were performed. The chemical composition of the material of the connecting rod was determined by optical emission spectrometry on the Belec Compact PORT HLC device. The obtained results were compared with the standard steel specification of the connecting rod. The specimen for a metallographic examination was sliced perpendicular to the longitudinal axis of the connecting rod, near the surface of the fracture. The preparation of the metallographic sample consisted of the standard procedures of grinding, polishing and etching with a suitable reagent. The grinding was performed on the grit sandpaper P150, P240, P320, P400, P600, P1200 and P2500, followed by the polishing, performed with the diamond paste 7/5 μm and 5/3 μm, respectively. The microstructure was developed by immersing the specimen into the solution of 5% Nital reagent.

The specimen was examined in the polished condition under the metallographic light microscope Leitz-Metalloplan, equipped with a camera system and software for image acquisition and data processing. The objective of the metallographic examination was to determine the material microstructure and reveal the presence of any imperfections that might have led to the failure. The macrostructure was developed by using deep etching on the mechanically prepared surface sample, in a 50% solution of hydrochloric acid, at the temperature of 80 degrees during 60 minutes, according to the requirements of the SORS 1710 standard. The tensile tests were conducted on the specimens taken from the big end of the connecting rod. The tensile tests were done according to the ASTM E8M-11 at the strain rate of 3.3×10-3 s-1 on the Shimadzu Servopulser testing machine. Hardness measurement was conducted by the HRC method. Also, on the cross-section of the connecting rod, the measuring of microhardness (HV 1) was implemented. The Rockwell (HRC) hardness tests were performed on the standard hardness test machine WILSON 2R. Vickers microhardness measurement was conducted by using the digitally controlled hardness test machine (HVS-1000), applying force of 9.807 N for 15 s.

Identification of stress concentration areas of the connecting rod was carried out by applying the finite element (FE) analysis in CATIA V5R22 Generative Structural Analysis Workbench. For this purpose, plausible 3D solid model of the connecting rod, was developed using CATIA V5R22. The maximum load of the connecting rod was applied.

3. Results

After removing the engine from the test bench, analysis of the engine assemblies and determination of damage was conducted. It was noticed:

- After removing the bottom part of the crankcase of the engine, it was concluded that there are no traces of damage on the engine cylinders. Also, the lower toothed gear was not damaged, except for the fact that, on the tachometer shaft the gear was thrown out of the contact with the drive gear at the time when a part of the connecting rod hit and tore off this part of the engine.
- Traces of leak at the injector of the first left cylinder were not found and the injector is fully functional. In this way, the suspicion that the irregular injection had led to the occurrence of the melting and damaging of the piston was eliminated.
- Inspection of combustion chamber surface in all cylinders has not revealed any irregularities in combustion processes.
- The first left piston with the part of the fractured connecting rod was removed without any resistance.
- When the high pressure pump was removed, together with the drive and manifold air, it was found that the part of the broken connecting rod had caused damage to the cylinder block. The ridge of the bottom part of the cylinder block, located between the cylinders, was fractured.
- After the removal of the cups of the main supporting bearings of the crankshaft, it was revealed that the bearings and the crankpin journals of the engine crankshaft were in good condition without any traces of damage.

After the above mentioned activities had been conducted and the analyses had been carried out, it was concluded that the main cause of the engine breakdown was the failure of the connecting rod, so more attention is paid to the determination of the fracture cause of the connecting rod itself.

3.1. Visual inspection

After dismounting the parts of the broken connecting rod from the piston and the crankpin journal crankshaft of the failed engine, the visual examination of the parts of the broken connecting rod was performed.

It was noticed that the fracture of the connecting rod occurred at a distance of approximately 15 cm from the center of the big end connecting rod, Fig. 3a.

The visual and the examination under the stereomicroscope showed the presence of significant macroscopic damage of fracture surfaces on the original fractured surface of the connecting rod, caused by the uncontrolled movement of the connecting rod after the catastrophic failure until the engine stopped running (Fig. 4).

The analysis of the fracture surface was carried out on the part of the connecting rod marked with “part II” in Fig. 3a. Neither position where the crack was initiated nor presence of the traces, pointing to the

possibility that the fracture was caused by the connecting rod fatigue, was seen. Significant damage to the fracture surfaces largely prevented a better analysis of the fracture surfaces.

The traces of machining on the external surface of the connecting rod were detected (Fig. 5). Also, in the radial transition between the flat surfaces, the presence of undercuts was observed. In those areas, the machining knife penetrated the radius and made a recess.

No undercuts were noticed at the cross section of the connecting rod body. The traces of machining on the connecting rod surface were confirmed by using the SEM microscope (Fig. 6).

3.2. Surface roughness

The surface roughness was measured on the marked area of connecting rod shown on Fig. 7. The average value of surface roughness (Ra) is 1,6 μm. This value, according to standard SRPS M.A1.026 [8], corresponds to the N7 class of surface roughness. According to the technical documentation, class roughness should be N1, which corresponds to the values Ra of 0.006 to 0.025 μm.

3.3. Metallography

The macrostructure of the sample is shown in Fig. 3b. The visible presence of the non-metallic inclusions, as well as the impermissible metallurgical defects, such as porosity, voids, cracks, bubbles etc. were not observed. No defects of the forging was detected.

The microstructure of the material is homogeneous, fine-grained and corresponds to the structure of the tempered martensite without the presence of the segregation (Fig. 8).

3.4. Microfractography

In order to obtain detailed information about mechanism that led to the failure, the fracture surfaces were observed by SEM. The observed fracture surfaces were significantly damaged, as a consequence of the uncontrolled movement of the parts of the broken connecting rod. These parts after had collided with the certain other parts of the engine until the moving parts of the engine stopped moving. Because of that, the failure mechanism cannot be determined with certainty. Further, on the small, undamaged parts of the fractured surface, the indicators (the lines of fatigue) pointing to the fatigue of the mechanism of the fracture were not detected. It should be highlighted that it is very hard to detect the lines of fatigue in martensitic and bainitic structures present here. No radial ridges that would indicate unstable crack propagation or the brittle character of the fracture were observed, either. On the other side, the results of the fracture surface analysis disclosed ductile character of the fracture.

In the zone of the radius of the connecting rod, in a very narrow band of the intact fracture surface, right next to the outer edge, the “stretch marks” were identified (Fig. 10). The presence and origin of the “stretch marks” cannot be explained with certainty, i.e. whether they occurred as the result of the fracture or possibly presented the traces of the fatigue of the material. The part of the sample of the connecting rod outside the area indicated by the red line was further compacted after the initiation of

the fracturing of connecting rod and no additional indicators that could point to the cause of the fracture can be seen.

3.5. Chemical composition

The results of the analysis of the chemical composition of the connecting rod are shown in Table 2.

The content of the major alloying elements (C, Cr, Ni) and the presence of Mo, corresponding to the chemical composition of the steel marked 18H2N4MA according to GOST 4543-71 [6].

3.6. Hardness measurements

The hardness of the connecting rod material was measured on the surface (Fig. 11) while the microhardness was measured on the cross section of the connecting rod (Fig. 12).

The results are shown in Table 3 and Table 4.

The values of hardness and microhardness are uniform, without significant mutual differences. The mean values of the surface macrohardness and the microhardness correspond to the tempered condition of the steel marked 18H2N4MA [6].

3.7. The finite element analysis

The continuum of the previously modeled 3D geometry of the connecting rod was meshed by the 4-nodes linear tetrahedral solid elements generating the FE model of 578,472 nodes and 367,226 elements.

The mechanical properties of the material, applied to the 3D geometry of the connecting rod, were taken for the alloy steel marked 18H2N4MA.

The typical values of the mechanical properties are about 1220 MPa for Yield Strength, 1330 MPa for the Ultimate Tensile Strength and 9.22% for elongation. The obtained values correspond to the requirements of the GOST 4543-71 standards and are consistent with those required mechanical properties. The resulting typical stress-strain diagram is shown in Fig. 13.

The forces of the engine mechanism of the subject-matter diesel engine are different for the main and the auxiliary engine cylinders (Fig. 14) due to the different kinematic magnitudes and weights of the moving parts of the engine.

For this reason, a calculation is made separately for the forces of the main cylinder and the auxiliary cylinder, after which the superimposing of these is performed on the crankpin journal of the engine

crankshaft. In this way, on each crankpin journal of the engine crankshaft, the resultant force is obtained from the corresponding cylinder (the main and the auxiliary).

The gas force F_{gg} and the inertial force F_{ig} of the straight-line oscillatory mass of the main piston act on the piston pin, which can be algebraically summed up since they are collinear, and in that way a resulting force on the piston pin F_{rg} is obtained [7]:

$$F_{rg} = F_{gg} + F_{ig} \quad [\mathrm{N}] \tag{1}$$

where:

$$F_{gg} = A_{kl} \cdot (p_g - p_k) = \frac{D_{kl}^{\,2}\pi}{4} \cdot (p_g - p_k) \ [\mathrm{N}] \tag{2}$$

$$F_{ig} = -a_g \cdot m_{og} \ [\mathrm{N}] \tag{3}$$

In the equations (2) and (3), certain symbols have the following meanings:

- A_{kl} - cross-sectional area of the piston [m^2],
- D_{kl} – the piston diameter [m],
- p_g – the pressure of the main cylinder [Pa],
- p_k – the gas pressure from the oil pan (close to atmospheric pressure) [Pa],
- a_g – the straight-line oscillatory mass of the main cylinder acceleration [m/s^2],
- m_{og} –the straight line oscillating mass of the main cylinder, which includes the weights of the piston, the piston rings, the piston pin, the wrist pin and the reduced mass of the main connecting rod [kg].

The resulting force on the piston is decomposed into the component perpendicular to the cylinder axis (normal force Ng) and the component in the direction of the axis of the main connecting rod (connecting rod force Kg):

$$N_g = F_{rg} \cdot tg\beta \ [\mathrm{N}] \tag{4}$$

$$K_g = \frac{F_{rg}}{\cos\beta} \quad [\mathrm{N}] \tag{5}$$

The force in the connecting rod acts on the crankpin journal and is decomposed into one component in the direction of the axis of the crankpin journal (the tangential force *Tg*) and another in the direction of the radius of crankshaft web (the radial force *Rg*). When the forces *Tg* and *Rg* are moved to the rotation axis of the crankshaft, the indicated torque (M_{ig}) originating from the main cylinder of the engine is obtained.

$$T_g = K_g \sin(\alpha + \beta) \quad [\text{N}] \tag{6}$$

$$R_g = K_g \cos(\alpha + \beta) \quad [\text{N}] \tag{7}$$

$$M_{ig} = T_g \cdot R \quad [\text{Nm}] \tag{8}$$

The force of the auxiliary connecting rod was not taken into account in determining the applicable load for the stress state of the main connecting rod because its influence is negligible. For the stress analysis of the connecting rod, the maximum force in the connecting rod previously calculated to be *Kg* = 160.000,00 [N], Fig. 15, was used.

The Kg maximum force was applied to the center of the small end of the connecting rod in the direction of the axis of the connecting rod, Fig. 14. The appropriate contact definitions have been assigned to the connecting rod. The nodes of the inner cylindrical surface of the big end of connecting rod were fixed by restraining all degrees of freedom. The displacements were free in the rest of the connecting rod.

The stress field of the connecting rod obtained according to the Von Mises criterion and the visualization of the Von Mises stress field patterns are shown in Fig. 16.

The analysis of the stress state of the connecting rod showed that the maximum value of stress of the connecting rod was 398,7 MPa, in the part of the connecting rod where the initiation of the fracture of the connecting rod was assumed to have been made.

4. The analysis of the results

The visual inspection of the parts and the assemblies of the disassembled engine did not answer the question of what had happened; no irregularities that might be the cause of the fracture of the connecting rod of the first left cylinder were observed. Therefore, attention in searching for the cause of the fracture was focused on the connecting rod.

The fractographic analysis could not confirm that the fatigue had been the main cause of the fracture of the connecting rod. Based on the observed “stretch marks” on the part of the radius of the fracture surface these cannot be said with certainty to be indicative of the fatigue since they did not have the shape characteristic for fatigue. It is not possible, either, to confirm with certainty whether they occurred as a result of the breakage or possibly represent the traces of the fatigue of the material.

The metallographic examinations did not reveal the presence of the metallurgical imperfections and defects in the material of the connecting rod. The chemical analysis of the material and the obtained

values of the mechanical properties have confirmed the values given in the standard specification of the steel marked 18H2N4MA.

On the sample surface, the traces of machining were observed. The undercuts and the sharp lines during the changeover from the flat side towards the lateral sides, in which the machining knife entered the radius, were also noticed. In the conditions of high cyclical variable loads, the perceived processing deficiencies represent the potential points where a crack can be initiated. In this regard, the observed presence of the discrete recess that extends along the entire length of the radial changeover from the flat side towards the lateral sides on the connecting rod is especially unfavorable.

In addition to the visible traces of machining, it is also observed that the level of the surface roughness is significantly higher than the level required in the technical documentation.

Increase of the surface roughness of the highly-loaded parts exposed to the high cyclical changes of the stress state may be one of the causes of a structural failure due to the dropping of the dynamic strength of the material and decreasing the crack initiation life [9,10].

This is supported by the observed inadequate level of the polishing of the surface of the connecting rod body. Namely, the microscopic record led to the observation of the fact that the outer rounding of the cross section of the connecting rod body designed as the “I” profile was not polished, as it is suggested in the technical documentation.

The initial point of fracture had probably occurred on one of the eight points of the convex rounding of the cross section of the body of the connecting rod, which is the position of the connecting rod with the maximum value of stress (398,7 MPa), according to the analysis of the stress state.

5. Conclusions

The maximum value of stress of the connecting rod at the location where fracture occurred and the higher level of surface roughness, which was additionally having an impact on the reduction in the dynamic strength of the connecting rod material, were identified as the main causes of the fracture of the connecting rod. Also, the breakage of the connecting rod was additionally influenced by the fact that the engine was running at maximum load for a long period of time.

In order to prevent breakage of the connecting rod in the future, it is recommended the followings:

- the radius of the rounding of the connecting rod body should be increased in the positions on the body of the connecting rod with the increased concentration of stress in order to reduce the concentration of the stress of the connecting rod;

- the polishing of the connecting rod should be scheduled within the framework of the final machining; and
- the control of making parts for the engine during serial production should be improved.

References

[1] Roger Rabb. Fatigue failure of a connecting rod. Engineering Failure Analysis, Vol. 3, No. 1, pp. 13-28, 1996.

[2] Bai-yan He, Guang-da Shi, Ji-bing Sun, Si-zhuan Chen, Rui Nie. Crack analysis on the toothed mating surfaces of a diesel engine connecting rod. Engineering Failure Analysis 34 (2013) 443–450.

[3] Khare S, Singh OP, Bapanna Dora K, Sasun C. Spalling investigation of connecting rod. Engineering Failure Analysis 19 (2012) 77–86.

[4] Griza S, Berton F, Zanon G, Reguly A, Strohaecker TR. Fatigue in engine connecting rod bolt due to forming laps. Eng Fail Anal 2009;16:1542–8.

[5] Son JH, Ahn SC, Bae JG, Ha MY. Fretting damage prediction of connecting rod of marine diesel engine. J Mech Sci Technol 2011;25:441–7.

[6] State Standard of the Russian Federation GOST 4543-71. Standard specifications for structural alloy steel bars; 1971.

[7] Spasić, V. Problem of IC engines crankshaft torsion oscillations. MSc Theses, Faculty of Mech. Eng., University of Belgrade, Belgrade 1990. (in Serbian).

[8] SRPS M.A1.026 Surface Roughness
Institute for Standardization of Serbia (2011) (www.iss.rs)

[9] N.A. Alang, N.A.Razak & A.K.Miskam. Effect of Surface Roughness on Fatigue Life of Notched Carbon Steel, International Journal of Engineering & Technology IJET-IJENS, Vol: 11, No. 01, pp. 160-163, February 2011.

[10] H. Itoga, K. Tokaji, M. Nakajima and H. Ko. Effect of Surface Roughness on Step-Wise S-N Characteristics in High Strength Steel. Int. J. of Fatigue, Vol. 25, pp. 379-385, 2003.

List of figures

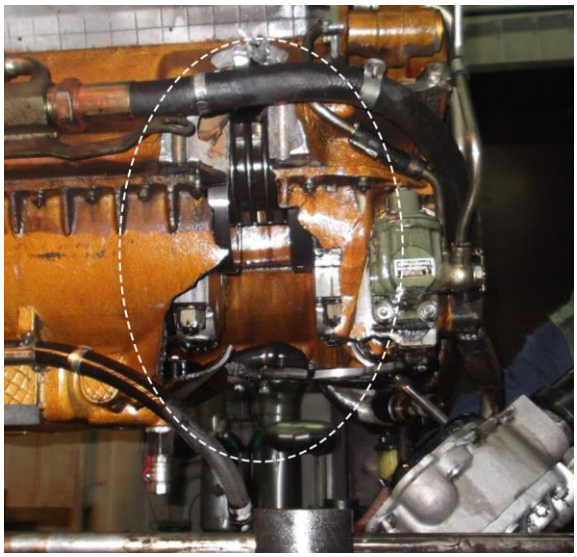

Figure 1

Figure 2

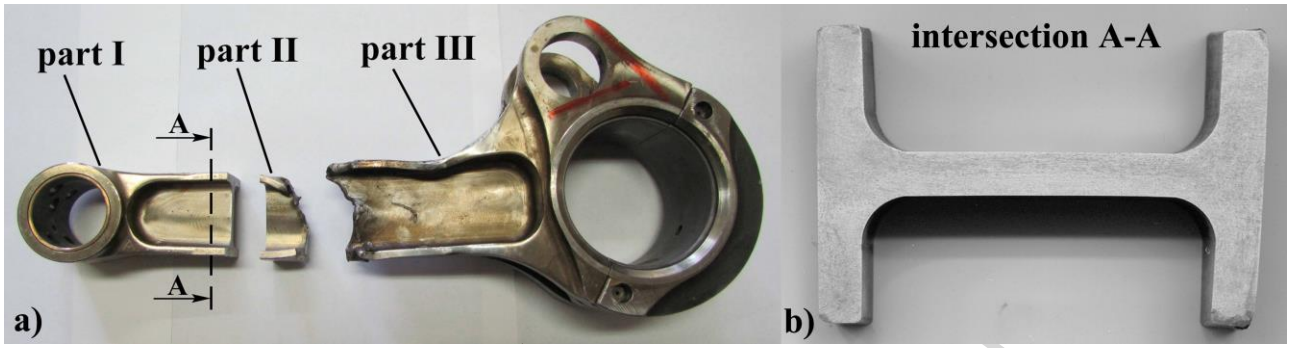

Figure 3

Figure 4

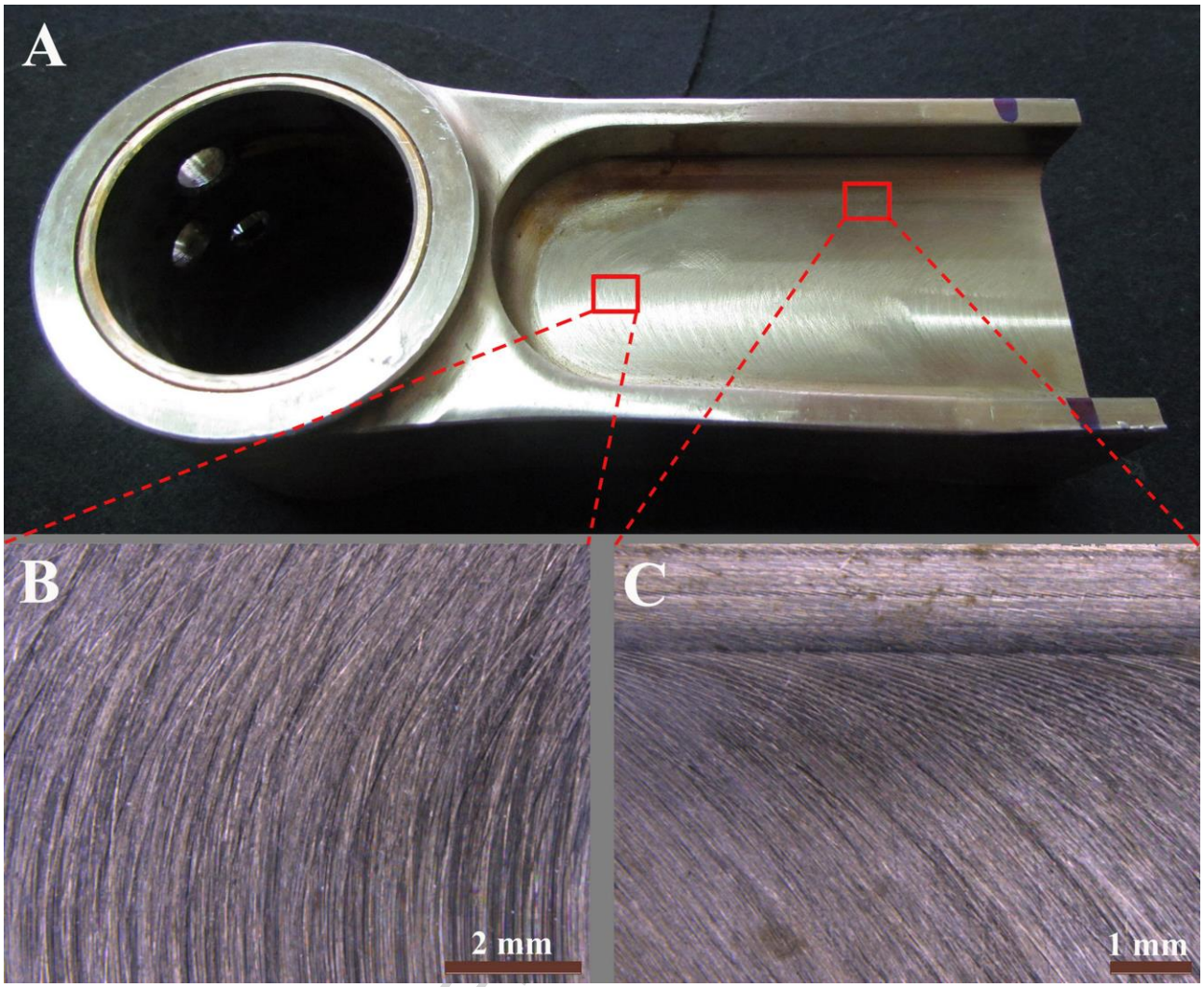

Figure 5

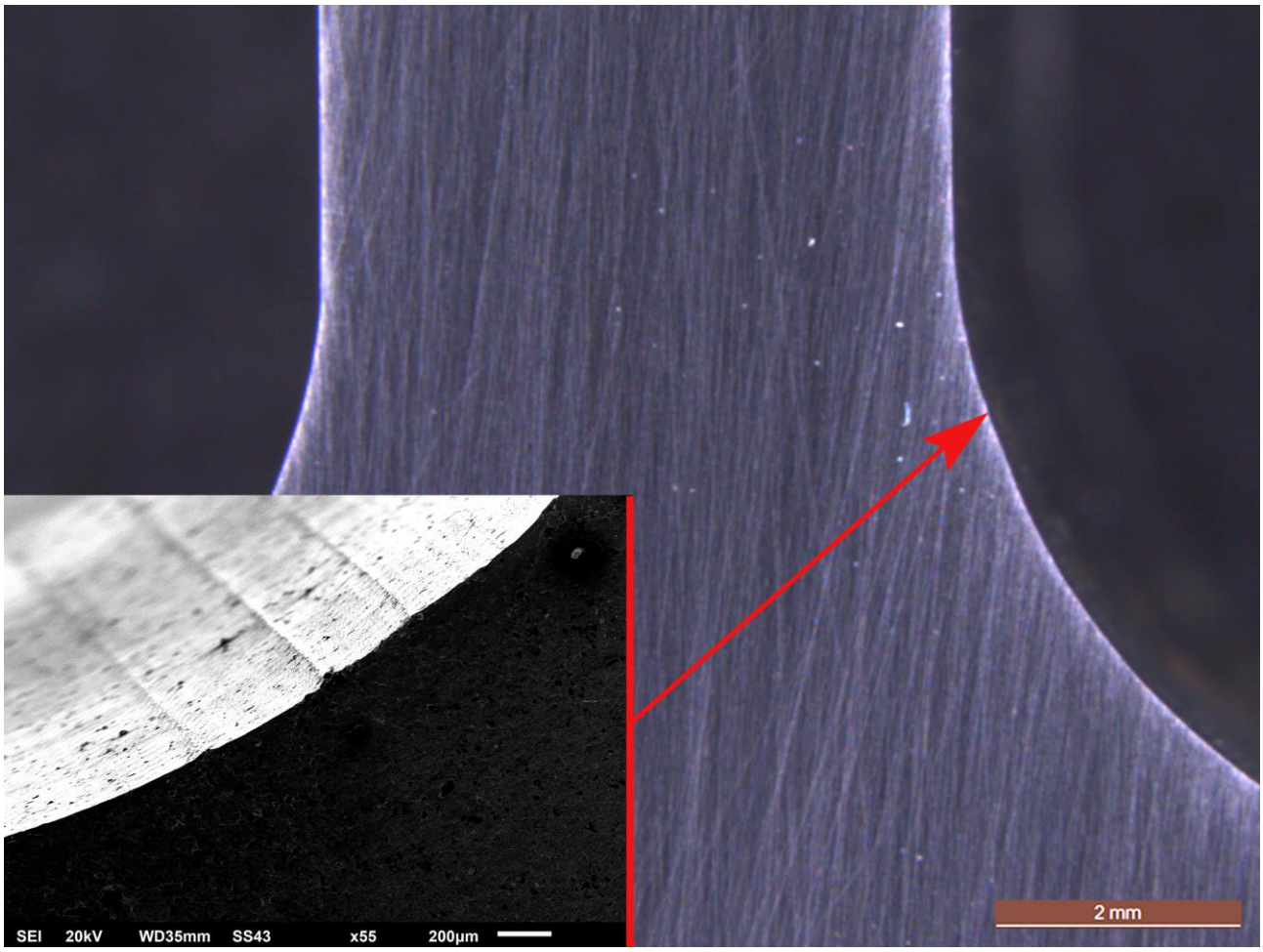

Figure 6

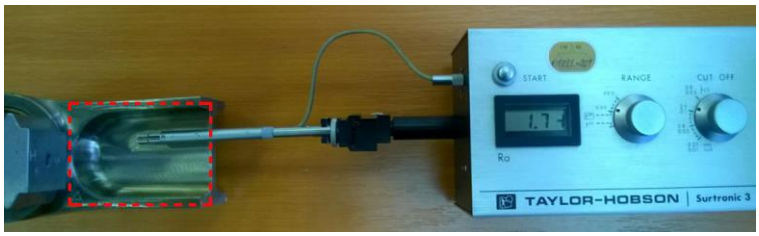

Figure 7

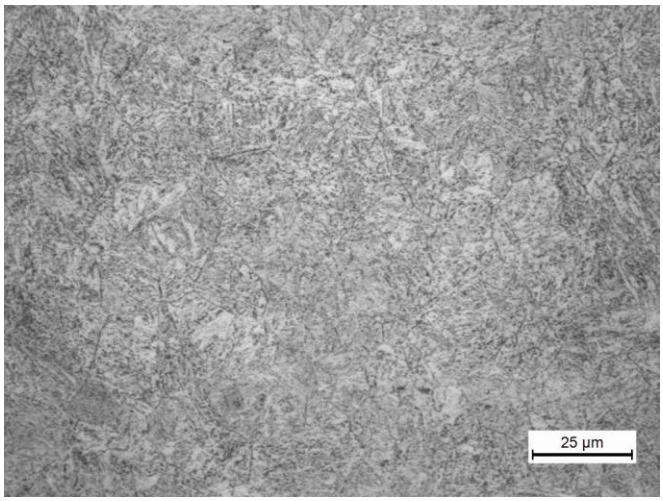

Figure 8

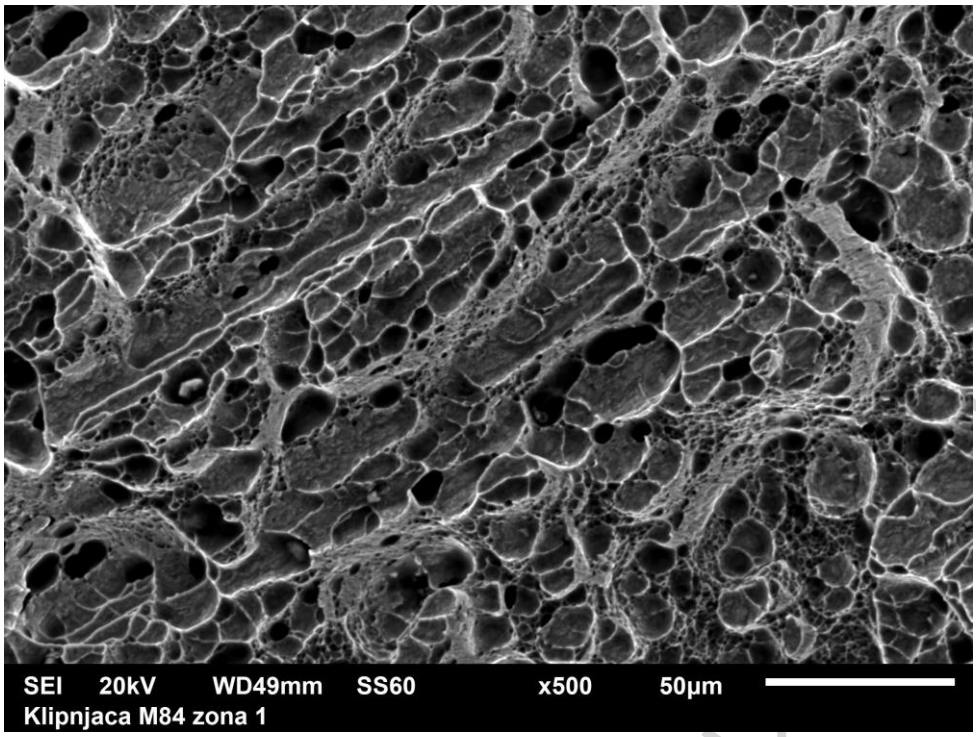

Figure 9

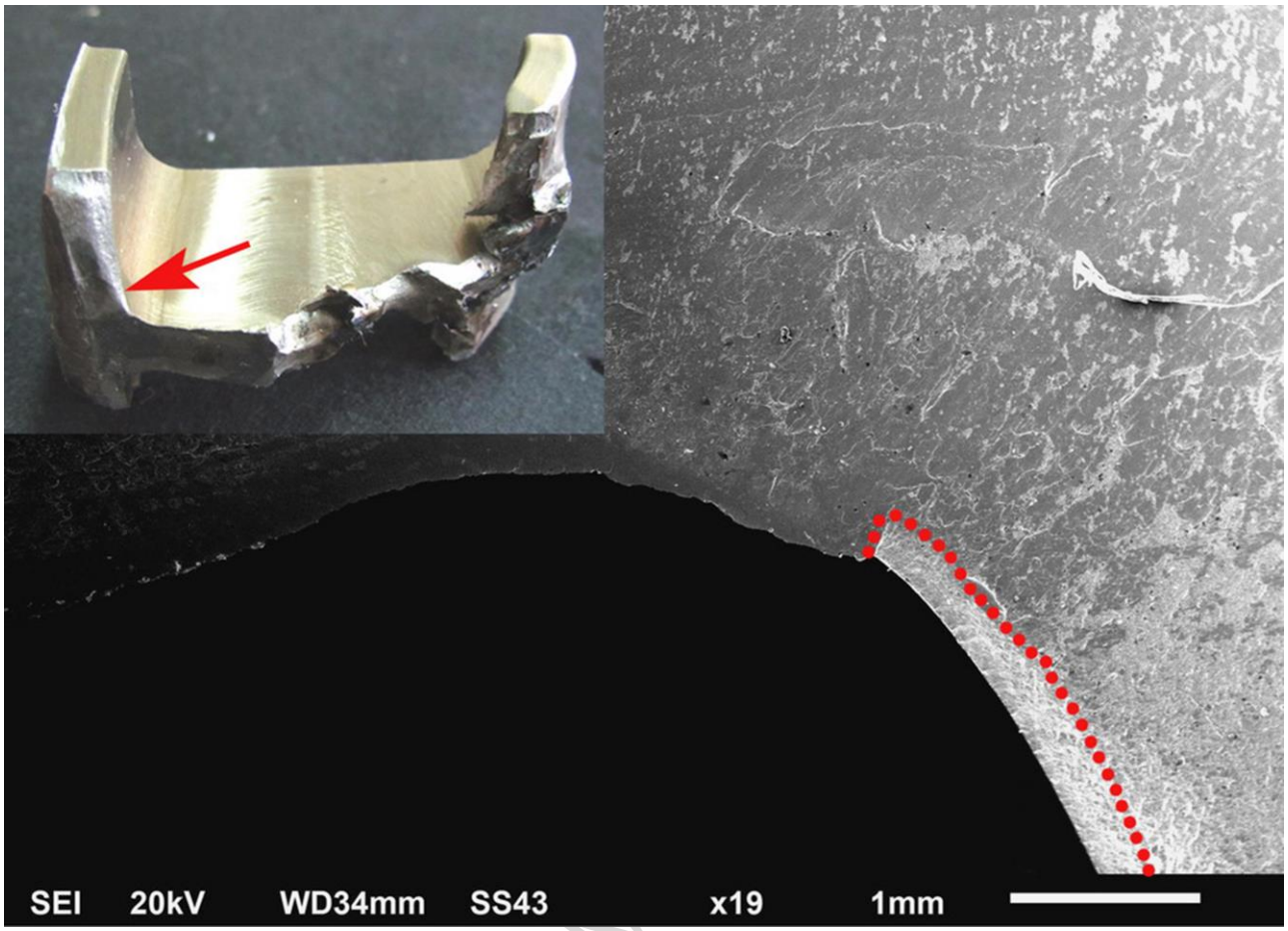

Figure 10

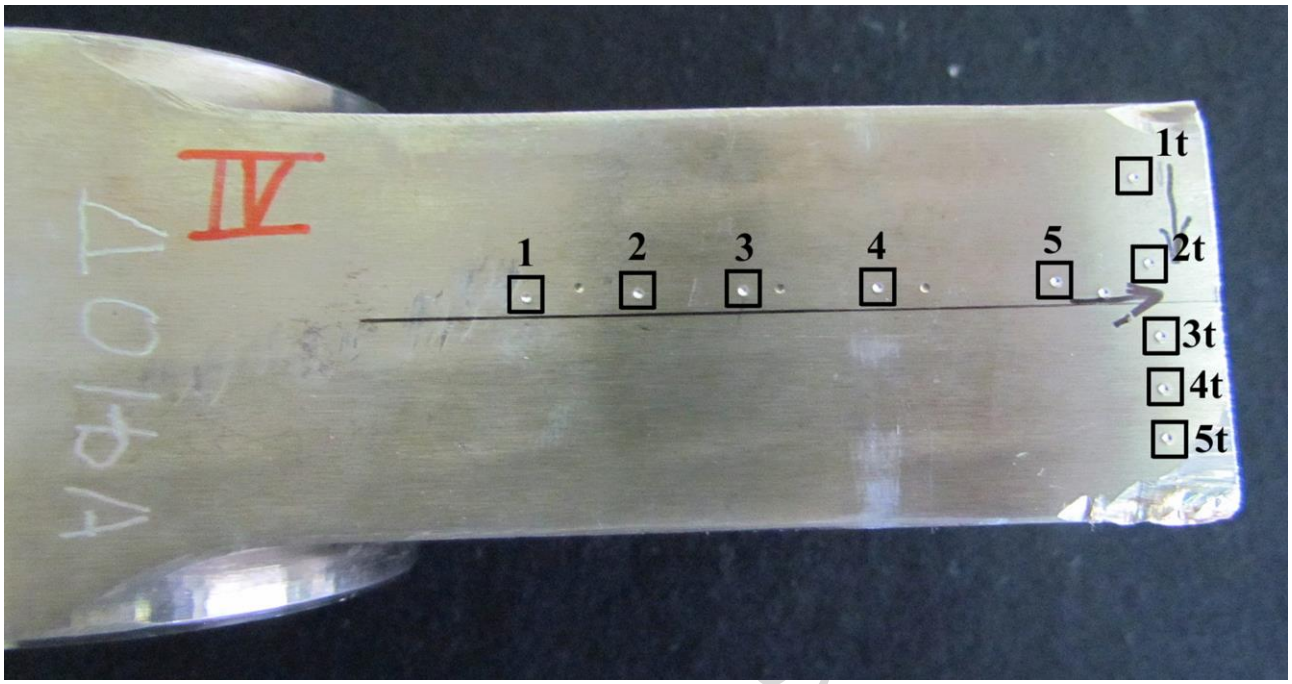

Figure 11

Figure 12

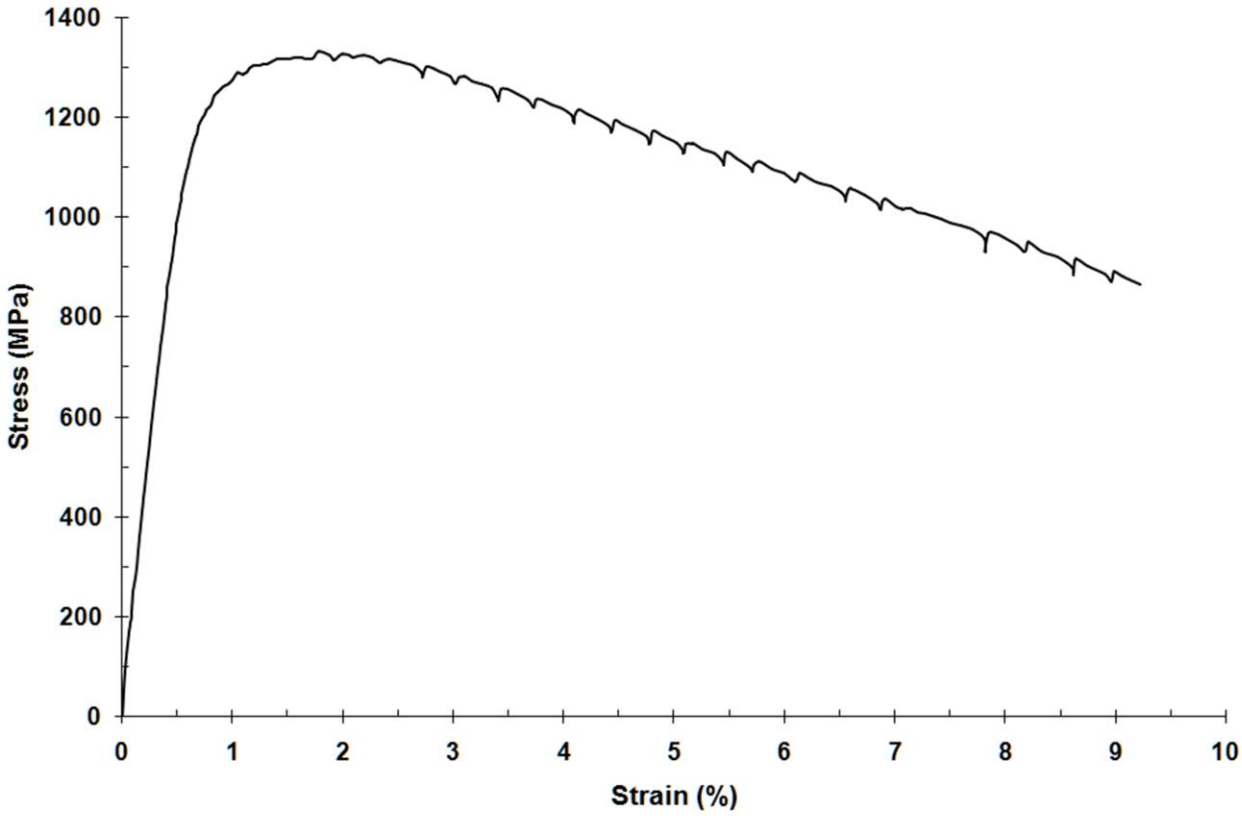

Figure 13

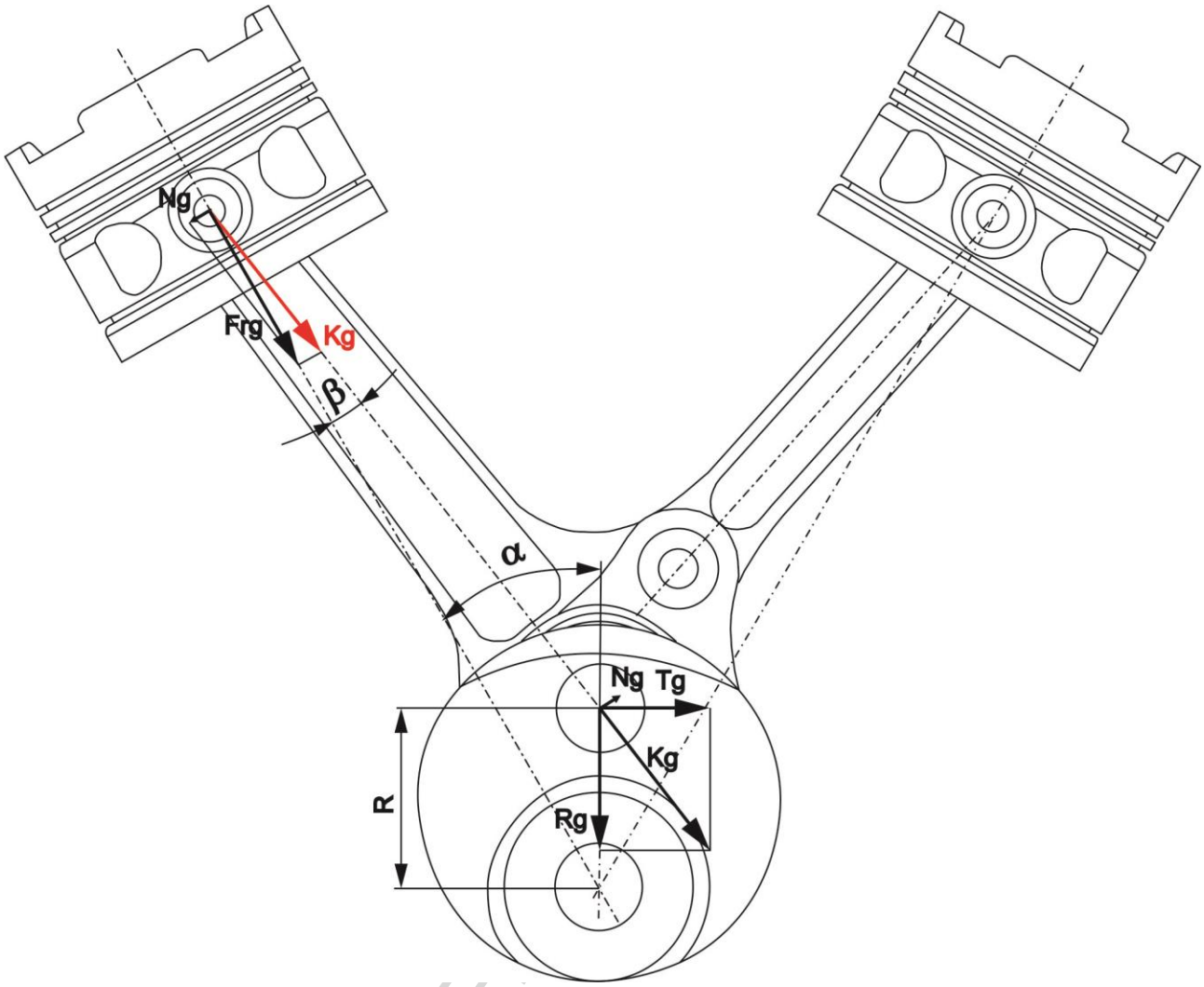

Figure 14

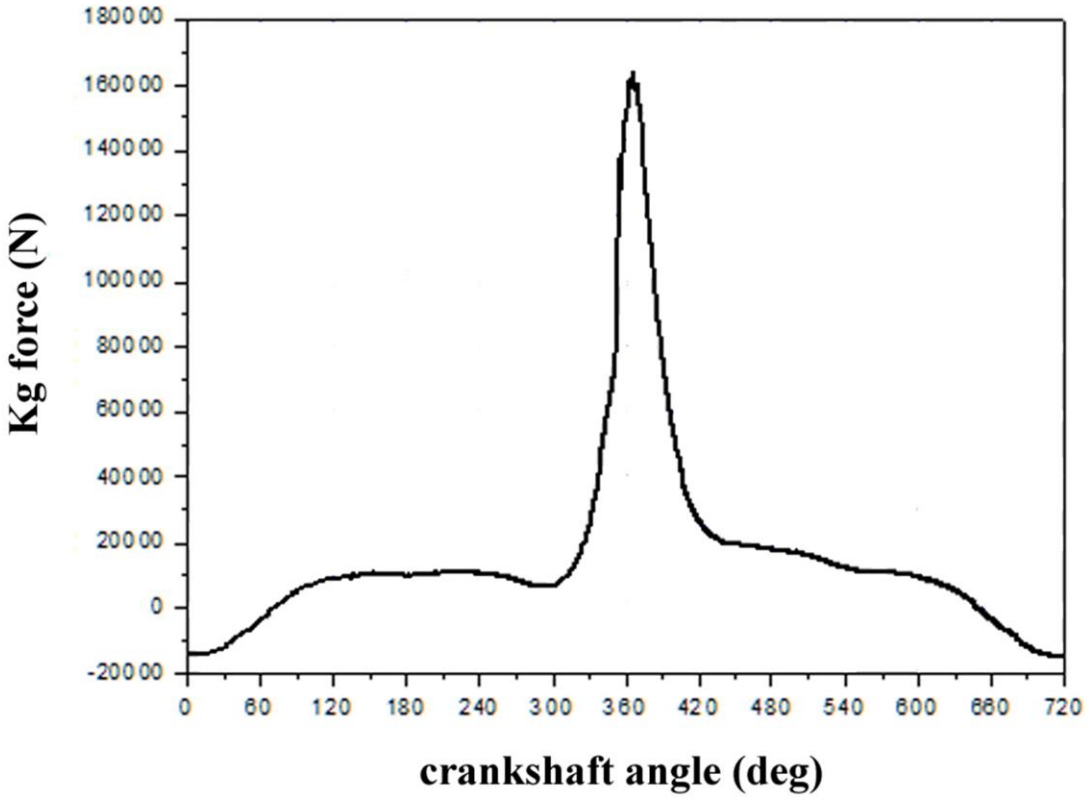

Figure 15

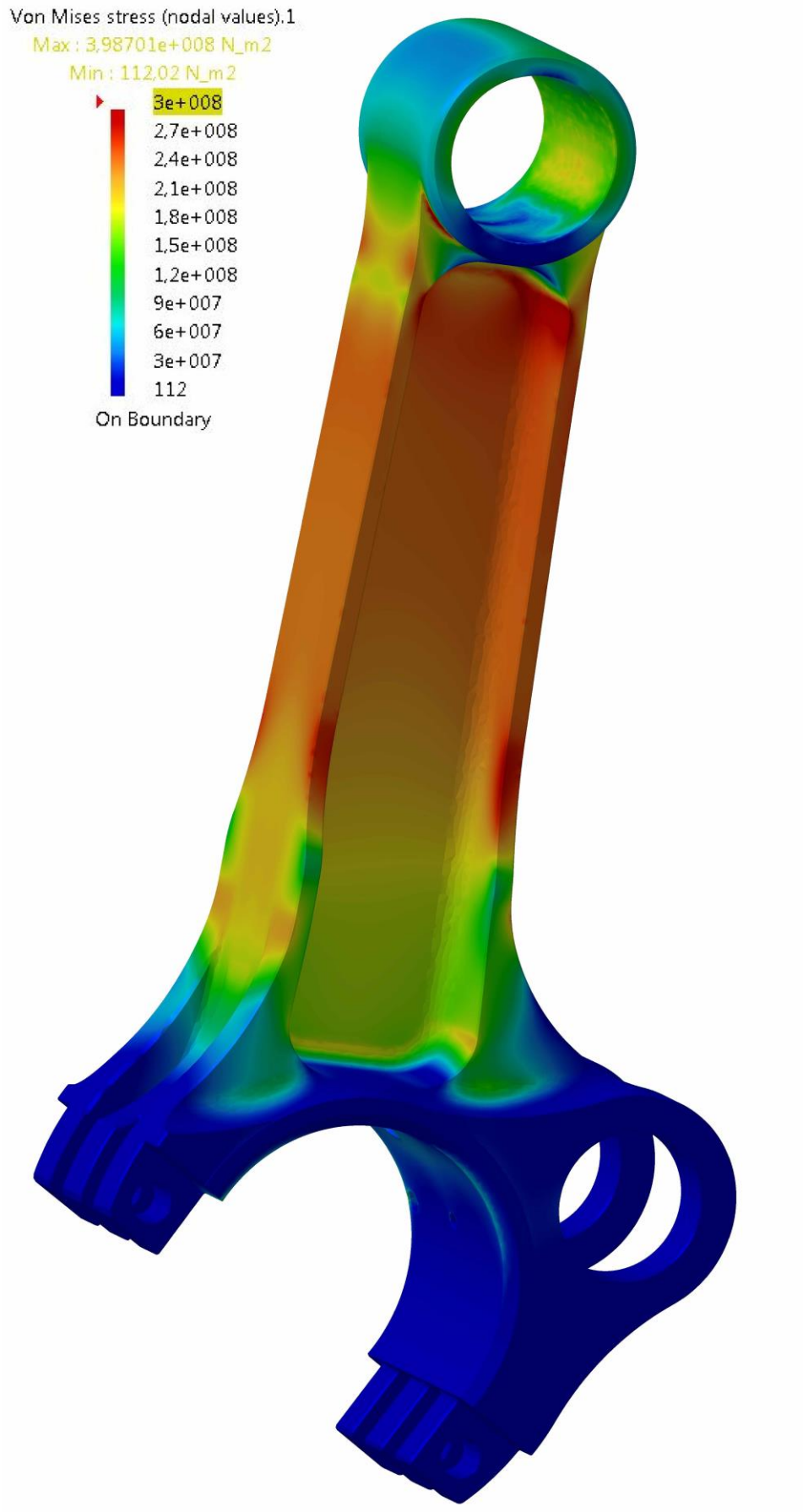

Figure 16

Failure analysis of a special vehicle engine connecting rod

Parameter	Value
Rated horsepower [hp]	1000
Rated speed [rpm]	2000
Bore [m]	0.150
Stroke length [m]	0.180
Volumetric displacement [L]	38,88
Number of cylinders	12
Weight [kg]	1090

Table 1. Engine specifications.

	Element								
	C	Si	Mn	Cr	Ni	Mo	P	S	Cu
Connecting rod	0.159	0.313	0.44	1.558	3.96	0.328	0.021	0.005	0.098
Standard specification for steel alloy 18H2N4MA	0.14-0.20	0.17-0.37	0.25-0.55	1.35-1.65	4.00-4.00	0.30-0.40	≤0.025	≤0.025	≤0.30

Table 2. Connecting rod chemical composition (wt.%).

	Measurement point									
	1	2	3	4	5	1t	2t	3t	4t	5t
Hardness (HRC)	38.5	37	37	37	33	36	36	33.5	36	38

Table 3. Hardness measurements.

	Microhardness HV1 *Measurement line*					
	A	A1	A2	A3	A4	A5
Mean value	398	389	387	382	397	400

Table 4. Average values of microhardness.

Highlights

- The connecting rod of the special vehicle engine fractured during the test.
- The finite element analysis showed the highest stress in the fracture origin area.
- The connecting rod material met the requirements of the standard specification.
- The bad machining of the connecting rod was observed.
- The absence of the polishing of the connecting rod was observed.